Histol Histopathol (2023) 38: 1283-1294

Histology and Histopathology
From Cell Biology to Tissue Engineering

ORIGINAL ARTICLE Open Access

D-mannose reduces adipogenesis by inhibiting the PI3K/AKT signaling pathway

Haozhi Lin[1], Xin Li[2], Jiping Zhao[3], Lei Wang[1], Yizhen Liu[1] and Cui Gao[2]

[1]Department of Stomatology, [2]Department of Neurology and [3]Department of Radiology, The Affiliated Hospital of Qingdao University, Qingdao University, Qingdao, Shan Dong Province, PR China

Summary. Purpose. To explore the effects and potential mechanisms of D-mannose on adipogenic differentiation of two kinds of representative mesenchymal stem cells (MSCs).

Methods. We cultured two kinds of representative MSCs, human adipose tissue-derived stromal cells (hADSCs) as well as human bone marrow mesenchymal stem cells (hBMSCs), with adipogenic-induced medium containing D-mannose or D-fructose as the control. Oil red O staining, quantitative real-time polymerase chain reaction (qRT-PCR), and western blot (WB) were used to detect whether D-mannose had effects on adipogenic differentiation of MSCs. RNA sequencing (RNA-seq) transcriptomic analysis was further used to explore the potential mechanisms of D-mannose on adipogenic differentiation of MSCs. After that, qRT-PCR and WB were used to verify the results of RNA-seq. Last, we removed bilateral ovaries of female rats to establish an estrogen deficiency obesity model, and gave D-mannose intragastric administration. One month later, the femurs of rats were sliced for oil red O staining, and the inhibitory effect of D-mannose on lipid formation *in vivo* was studied.

Results. Oil red O staining, qRT-PCR and WB *in vitro* demonstrated that D-mannose inhibited the adipogenic differentiation of both hADSCs and hBMSCs. Oil red O staining of femur sections proved that D-mannose was able to reduce *in vivo* adipogenesis. The results of RNA-seq transcriptomic analysis revealed that the adipogenesis-inhibition effects of D-mannose were performed by antagonizing the PI3K/AKT signaling pathway. Besides, qRT-PCR and WB further verified the results of RNA-seq.

Conclusion. Our study indicated that D-mannose was able to reduce adipogenic differentiation of both hADSCs and hBMSCs by antagonizing the PI3K/AKT signaling pathway. D-mannose is expected to be a safe and effective treatment strategy for obesity.

Key words: D-mannose, Adipogenesis, hADSCs, hBMSCs, Obesity, PI3K/AKT

Corresponding Author: Cui Gao, Department of Neurology, The Affiliated Hospital of Qingdao University, Qingdao University, Qingdao 266021, Shan Dong Province, PR China. e-mail: 1358550488@qq.com
www.hh.um.es. DOI: 10.14670/HH-18-631

Introduction

Adipose tissue plays a crucial role in energy storage, heat production and metabolism (Aherne and Hull, 1966; Green and Meuth, 1974). However, abnormal excessive accumulation of adipose tissue leads to obesity, which has become a global epidemic, and obesity is associated with diabetes, cardiovascular diseases, cancer, and other diseases (Piche et al., 2020; Rathmell, 2021). Obesity is closely associated with an excess of adipose tissue-derived stem cells or mesenchymal stem cells and adipogenesis subsequently (Ghaben and Scherer, 2019). Healthy diet habits and increased exercise are recommended as optimal first-line treatments for obesity, but usually fail to produce unremitting results due to poor individual self-control, reduced energy expenditure, and increased appetite under modern social pressures (Jackson et al., 2015). Medication is used as an adjuvant therapy to behavior change, especially when lifestyle changes do not generate the desired weight loss. However, there are some potentially harmful side effects of medication, such as cardiovascular events, nausea, vomiting, and diarrhea (Haywood and Sumithran, 2019).

D-mannose, an epimer of D- glucose, naturally exists in all kinds of fruits plants, and is a safe health-beneficial food supplement (Wang et al., 2021a). Abundant studies have revealed that D-mannose was able to suppress recurrent urinary tract infections by preventing E. coli from attaching to the urothelium (Kyriakides et al., 2021; Murina et al., 2021; Wang et al., 2021a). Zhang et al. proved that D-mannose suppressed autoimmune diabetes by upregulating regulatory T cells (Zhang et al., 2017). Zhou et al. demonstrated that D-mannose suppressed osteoarthritis by suppressing ferroptosis of chondrocyte (Zhou et al., 2021). Guo et al. reported that D-mannose enhanced periodontal ligament

stem cell immunomodulation through inhibiting IL-6 secretion (Guo et al., 2018). Besides, Sharma et al. demonstrated that D-mannose was able to improve host metabolism and prevent diet-induced obesity via altering host gut microbiome (Sharma et al., 2018). All these above results imply that D-mannose seems to regulate adipogenesis, but the potential molecular mechanism remains obscure. If D-mannose, the safe health-beneficial food supplement, could inhibit adipogenic differentiation of mesenchymal stem cells, it would be a promising strategy for treating obesity.

Materials and methods

Cell culture

Human adipose tissue-derived stromal cells (hADSCs) and human bone marrow mesenchymal stem cells (hBMSCs) were purchased from ScienCell Research Laboratories (San Diego, CA, USA). Fetal bovine serum (FBS), dulbecco's modified eagle medium (DMEM), α-minimum essential medium (α-MEM), 100x penicillin/streptomycin mixture and adipogenic inducible components mentioned below were purchased from Gibco (Grand Island, NY, USA). Both hADSCs and hBMMSCs were cultured at 37°C and 5% CO_2 atmosphere. 10% FBS and 1x penicillin/streptomycin were added in DMEM (hADSCs) or α-MEM (hBMMSCs).

Adipogenic differentiation under D-mannose or D-fructose treatment

hADSCs and hBMSCs were seeded into 6-well plates and then were divided into four groups, respectively: 1) PM: As mentioned above, cells in the PM group were cultured in DMEM or α-MEM containing 10% FBS and penicillin/streptomycin. 2) AM: cells were cultured in adipogenic medium in which was added 10 μM insulin, 100 nM dexamethasone, 200 μM indomecin, 500 μM 3-isobutyl-1-methylxanthine (IBMX) based on PM. 3) Mannose: 25 mM D-mannose was added based on AM. The concentration of D-mannose was referred to in the previous literature (Zhang et al., 2017; Liu et al., 2020a,b). 4) Fructose: 25 mM fructose was added based on AM.

Oil red O staining of cells

After adipogenic induction for 21 days, the cells were fixed with 4% paraformaldehyde for 1 hour and then stained with 0.3% oil red O (Sigma-Aldrich, St. Louis, MO) working solution. Microscopy was used to observe and photograph the lipid droplets in cells. Cells were then eluted with 100% isopropanol and quantified by spectrophotometry at 520 nm for oil red O.

Quantitative real-time PCR

Total RNA was extracted using the Qiagen RNeasy Mini kit (Qiagen, Hilden, Germany) after cells were adipogenic induced for 14 days according to the manufacturer's protocol. Then reverse-transcription kit (Takara, Kyoto, Japan) was used to synthesize complementary deoxyribonucleic acid (cDNA). The 7500 Real-Time PCR System (Applied Biosystems, Foster City, CA, USA) was used to assess the relative abundance of the cDNA and the thermal settings were used: 95°C for 10 min, 95°C for 15 s for 40 cycles and 60°C for 1 min. Glyceraldehyde-3-phosphate dehydrogenase (GAPDH) was used as a reference gene. The primers used are listed in Table 1.

Table 1. Sequences of the primers used in qRT-PCR.

Gene		Sequence	Amplicon size (bp)	TM (°C)
PPARγ	Forward primer (5′ to 3′)	GAGGAGCCTAAGGTAAGGAG	20	56.12
	Reverse primer (5′-3′)	GTCATTTCGTTAAAGGCTGA	20	53.94
C/EBPα	Forward primer (5′ to 3′)	GGGCCAGGTCACATTTGTAAA	21	58.76
	Reverse primer (5′-3′)	AGTAAGTCACCCCCTTAGGGTAAGA	25	62.02
FABP4	Forward primer (5′ to 3′)	TGGGAACCTGGAAGCTTGTCTC	22	58.76
	Reverse primer (5′-3′)	GAATTCCACGCCCAGTTTGA	20	62. 20
FOXO1	Forward primer (5′ to 3′)	AAGAGCGTGCCCTACTTCAA	20	59.31
	Reverse primer (5′-3′)	TTCCTTCATTCTGCACACGA	20	57.46
FOXO3	Forward primer (5′ to 3′)	GGTGCGTTGCGTGCCCTACT	20	65.76
	Reverse primer (5′-3′)	CCGTGGCAGTTCCACCGTGC	20	66.60
AKT	Forward primer (5′ to 3′)	GGGCCAGGTCACATTTGTAAA	21	58.76
	Reverse primer (5′-3′)	AGTAAGTCACCCCCTTAGGGTAAGA	25	62.02
β- actin	Forward primer (5′ to 3′)	CTCCATCCTGGCCTCGCTGT	20	64.13
	Reverse primer (5′-3′)	GCTGTCACCTTCACCGTTCC	20	61.23
GAPDH	Forward primer (5′ to 3′)	GAAGGTGAAGGTCGGAGTC	19	57.18
	Reverse primer (5′-3′)	GAAGATGGTGATGGGATTTC	20	53.72

Tm: melting temperature.

Western blotting analysis

To evaluate adipogenesis, total protein was extracted after cells were adipogenic induced for 14 days and then they were lysed in radioimmunoprecipitation assay (RIPA) lysis for 30 min at 4°C. Cell lysates were centrifuged at 14000 g for 30 min at 4°C. The total protein was tested by BCA protein assay kit (Thermo Fisher Scientific, Massachusetts, US) and was added to 10% PAGE. Polyvinylidene fluoride membranes (Millipore, Billerica, MA, USA) were blocked in 5% milk for 1 hour and then incubated with anti-PPARγ (Abcam, Cambridge, UK, 1:1000); anti-AKT (Abcam, Cambridge, UK, 1:1000); anti-pAKT (Abcam, Cambridge, UK, 1:1000); anti-PI3K (Abcam, Cambridge, UK, 1:1000) and anti-pPI3K (Abcam, Cambridge, UK, 1:1000) overnight at 4°C. Then membranes were incubated with secondary antibody solution for 1 hour at room temperature. ECL kit (CWBIO, Beijing, China) was used to detect the immunoreactive protein bands. The gray value of WB strip was quantitatively counted by Image J software (National Institutes of Health, USA).

RNA Sequencing

Total cellular RNA was extracted and the RNA sequencing system (Wayen Biotechnologies, Shanghai, P. R. China) was applied to explore the RNA expression. First, the RNA library was constructed through the QIAseq RNA Library Kit. Next, the raw fastq data quality was handled by the Cutadapt version 4.0 (Python Software Foundation, Amsterdam, Netherlands), perl5 version 5.26 (Sun Microsystems, Santa Clara, California, USA), and bowtie version 2.2.9 (Cognos, Baltimore, Maryland, USA) software. Genes with FPKM (fragments per kilobase of exon model per million mapped fragments)<0.1 in both the control and experimental group were ignored in the subsequent analysis. Gene ontology (GO) was performed by R package cluster Profiler. Meanwhile, the differentially expressed genes were identified by the edgeR program version 3.30.0 (Bioconductor, Boston, Massachusetts, USA). qRT-PCR was performed to confirm the expression levels of representative differentially expressed genes.

Ovariectomy Operations

The Animal Care and Use Committee of Qingdao University Health Science Center approved all animal experiments (approval number: LA2020009; Qingdao, China). 8-week-old (n=40) female Sprague Dawley (SD) rats were purchased from Spife Biotechnology Inc (Beijing, China) and randomly divided into 4 groups: 1): Sham: Rats were anesthetized, and the abdomen was cut open and sutured to simulate a sham ovariectomized operation. 2) OVX: Rats were anesthetized, and then bilateral ovaries were removed as described previously (Ducy et al., 1996). 3) Mannose: Ovariectomized rats were administered D-mannose (1.1 M) by gavage (2 mL each time, once a day). 4) Fructose: Ovariectomized rats were administered D- fructose (1.1 M) by gavage (2 mL each time, once a day).

The staining and quantification of oil red O of femurs

1 week after being fixed in 4% paraformaldehyde, the rat femur specimens were soaked in 10% ethylenediaminetetraacetic acid (EDTA) decalcification solution on 37°C shaker for 4 weeks. 5-mm-thick-sections were stained with oil red O to observe the histological morphology. The area of adipocytes and adipocyte area/tissue area based on H&E staining of femurs in 4 group rats were counted by Image J software (National Institutes of Health, USA).

Results

D-mannose inhibited adipogenic differentiation of hADSCs

As shown in Fig. 1A, in the AM group, a large number of lipid droplets appeared in the cells after adipogenic induction for 14 days, while in the Mannose group, there were significantly fewer lipid droplets. Interestingly, D-fructose at the same concentration as D-mannose did not inhibit the formation of lipid droplets in the cells in Fructose group. The quantitative results of oil red O staining also further confirmed the staining results (P<0.01, Fig. 1B). The results of qRT-PCR showed that in the AM group, the relative expression of adipogenic signature genes, including peroxidase proliferator-activated receptor-γ (*PPARγ*), CCAAT/enhancer binding protein α (*C/EBPα*), and fatty acid binding protein 4 (FABP4) were significantly increased after 14 days of adipogenic induction, while D-mannose significantly inhibited these adipogenic-relating genes (P<0.01, Fig. 1C). However, D-fructose in the same concentration as D-mannose in the control group had no significant inhibitory effect on adipogenic differentiation of hADSCs. Besides, the results of WB revealed that D-mannose was able to further inhibit the expression of adipogenic representative protein PPARγ (P<0.05, P<0.01, Fig. 1D, Fig. 1E).

D-mannose inhibited adipogenic differentiation of hBMSCs

The results of hBMSCs were consistent with those of hADSCs. In brief, D-mannose significantly inhibited the formation of lipid droplets but fructose did not exhibit this effect (Fig. 2A). The quantitative results of oil red O staining also further confirmed the staining results (P<0.01, Fig. 2B). The results of qRT-PCR showed that the relative expression of adipogenic signature genes, including *PPARγ*, *C/EBPα*, and *FABP4* were significantly increased after 14 days of adipogenic

induction in the AM group, while D-mannose significantly inhibited these adipogenic-relating genes in the Mannose group ($P<0.05$, $P<0.01$, Fig. 2C). Consistent with the result of hADSCs, D-fructose in the control group exhibited no significant inhibitory effect on adipogenic differentiation of hBMSCs. And the results of WB further proved that D-mannose further inhibited the expression of adipogenic representative protein PPARγ (**$P<0.01$, Fig. 2D,E).

D-mannose inhibited adipogenic differentiation of hADSCs and hBMSCs through the PI3K/AKT signal pathway

To explore the potential mechanisms of D-mannose, RNA-seq was used. As shown in Fig. 3A, 219 genes were upregulated and 226 genes were downregulated in volcano plot figure after D-mannose administration in the Mannose group compared with the AM group.

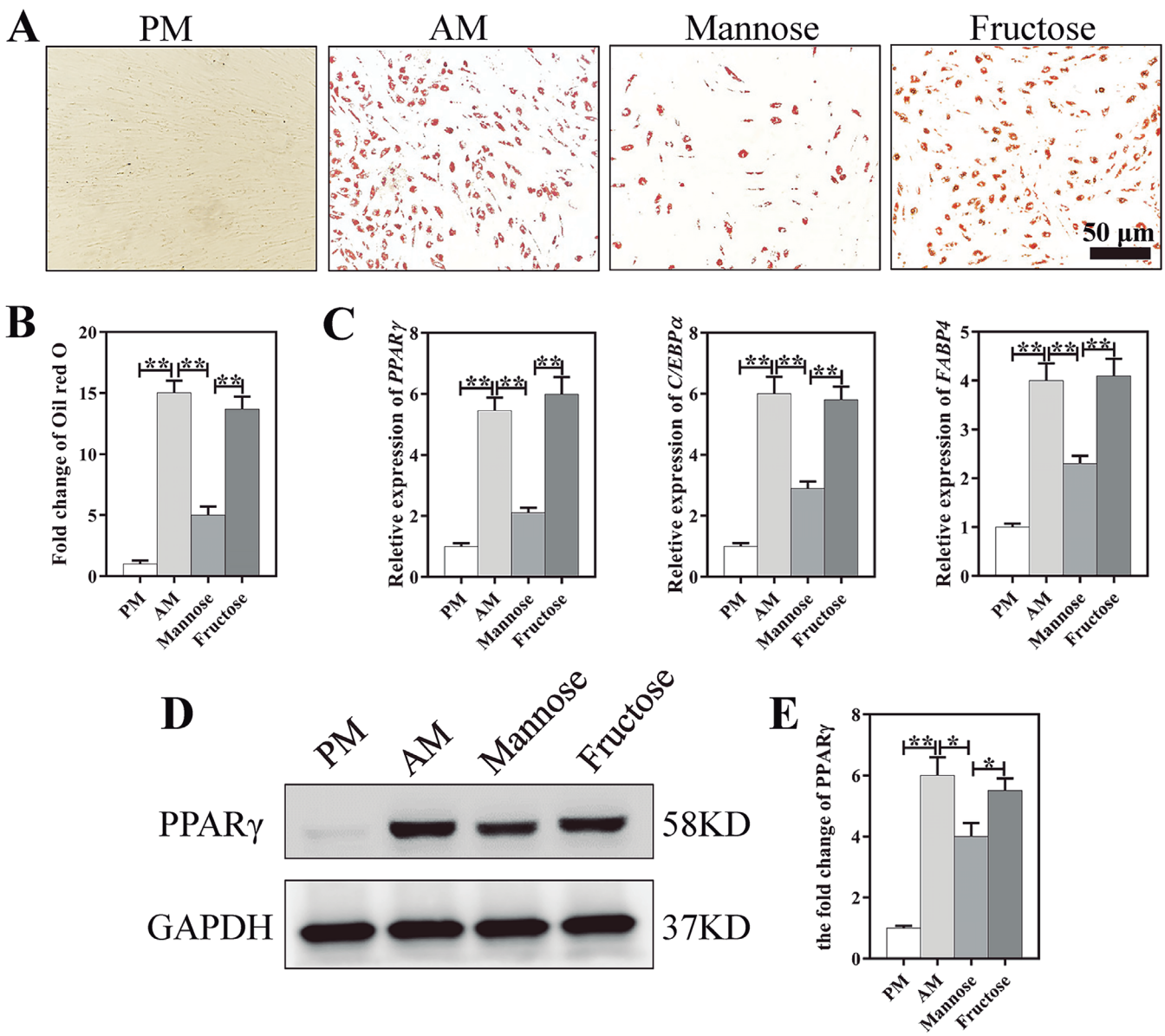

Fig. 1. D-mannose inhibited adipogenic differentiation of hADSCs. **A.** Representative images of oil red O staining in 4 groups. **B.** Relative quantitative results of oil red O staining. **C.** Relative adipogenic gene expression of PPARγ, C/EBPα, and FABP4 for hADSCs treated with 25 mM D-mannose or D-fructose. **D.** Western blot figures of adipogenic protein expression for hADSCs treated with 25 mM D-mannose or D-fructose. **E.** The fold change of the expression of PPARγ. *$P<0.05$, **$P<0.01$. hADSCs: human adipose tissue-derived stromal cells; PM: preliminary medium; AM: adipogenic medium; PPARγ: peroxidase proliferator-activated receptor γ; C/EBPα: CCAAT/enhancer binding protein α; FABP4: fatty acid binding protein 4. Scale bar: 50 μm.

Further GO gene enrichment results demonstrated that the differential genes were clustered in the PI3K/AKT signal pathway (Fig. 3B).

Then qRT-PCR was used to verify the expression of these differential genes in hADSCs ($P<0.05$, $P<0.01$, Fig. 4A) and hBMSCs ($P<0.05$, $P<0.01$, Fig. 5A) contained in the PI3K/AKT signal pathway, including *AKT*, forkhead box protein 1 (*FOXO1*), and forkhead box protein 3 (*FOXO3*). Consistent with the result of RNA-seq, in both hADSCs and hBMSCs, D-mannose obviously inhibited the relative expression of the target genes of *AKT*, *FOXO1* and *FOXO3*. In addition, the phosphorylation of PI3K and AKT as well as p-PI3K/PI3K and p-AKT/AKT were downregulated in both hADSCs ($P<0.05$, $P<0.01$, Fig. 4B,C) and hBMSCs ($P<0.05$, $P<0.01$, Fig. 5B,5C). Furthermore, Fig. 6 exhibited the mechanism diagrammatic drawing of D-mannose inhibited

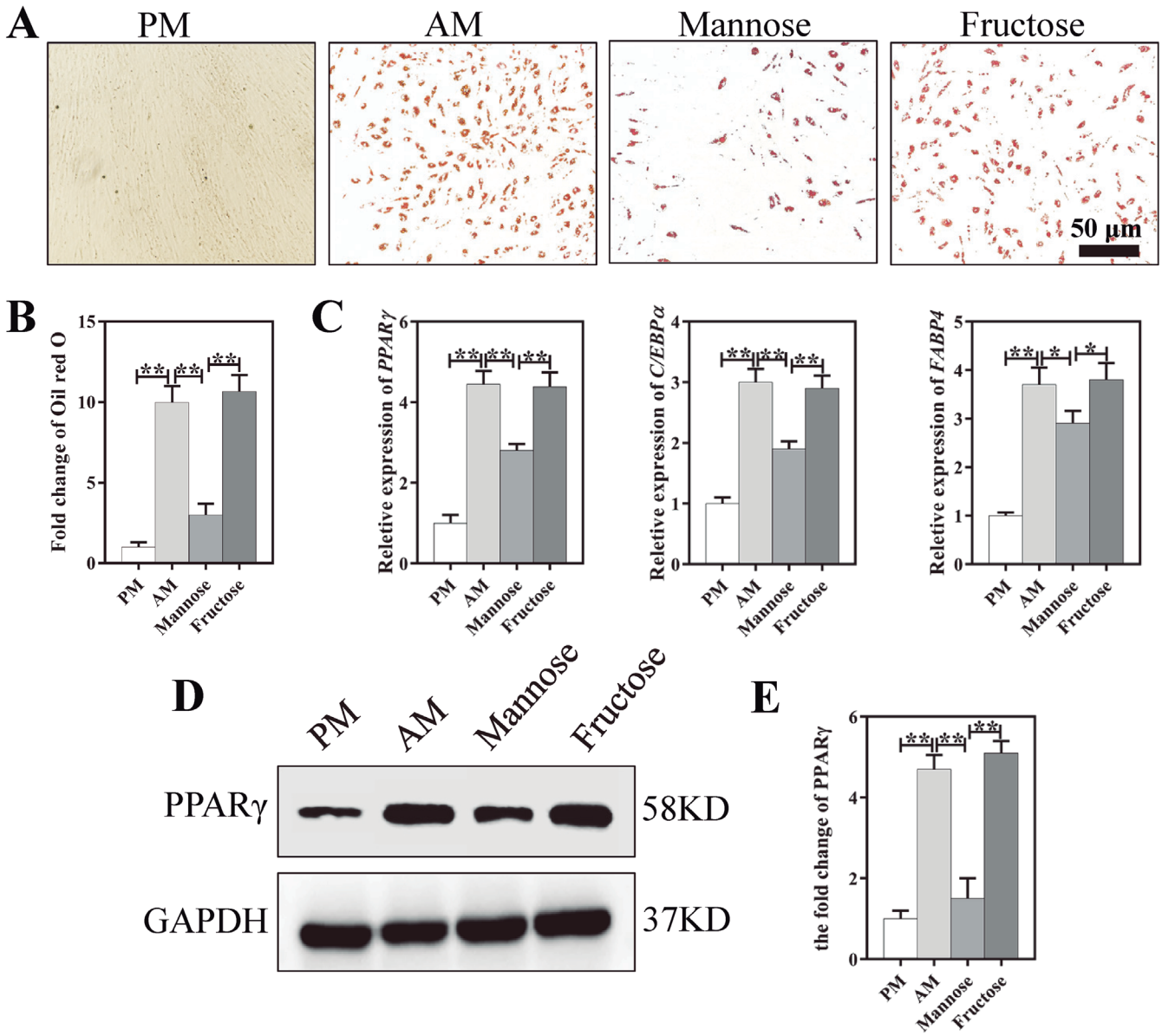

Fig. 2. D-mannose inhibited adipogenic differentiation of hBMSCs. **A.** Representative images of oil red O staining of hBMSCs in 4 groups. **B.** Relative quantitative results of oil red O staining. **C.** Relative adipogenic gene expression of PPARγ, C/EBPα, and FABP4 for hBMSCs treated with 25 mM D-mannose or D-fructose. **D.** Western blot figures of adipogenic protein expression for hBMSCs treated with 25 mM D-mannose or D-fructose. **E.** The fold change of the expression of PPARγ. **P*<0.05, ***P*<0.01. hBMSCs: human bone marrow mesenchymal stem cells; AM: adipogenic medium; PPARγ: peroxidase proliferator-activated receptor γ; C/EBPα: CCAAT/enhancer binding protein α; FABP4: fatty acid binding protein 4. Scale bar: 50 μm.

PI3K/AKT signal pathway.

D-mannose inhibited in vivo adipogenesis

To further investigate the effect of D-mannose on adipogenesis *in vivo*, female SD rats were ovariectomized to mimic estrogen deficient adipogenesis and were administered with D-mannose by gavage for 4 weeks. As shown in Fig. 7, there were more lipid droplets stained red by oil red O in the femur sections of rats in the OVX group, while the lipid droplets in the femur of rats in the Mannose group were reduced. Besides, the area of adipocytes and adipocyte area/tissue area based on H&E staining in OVX group were higher

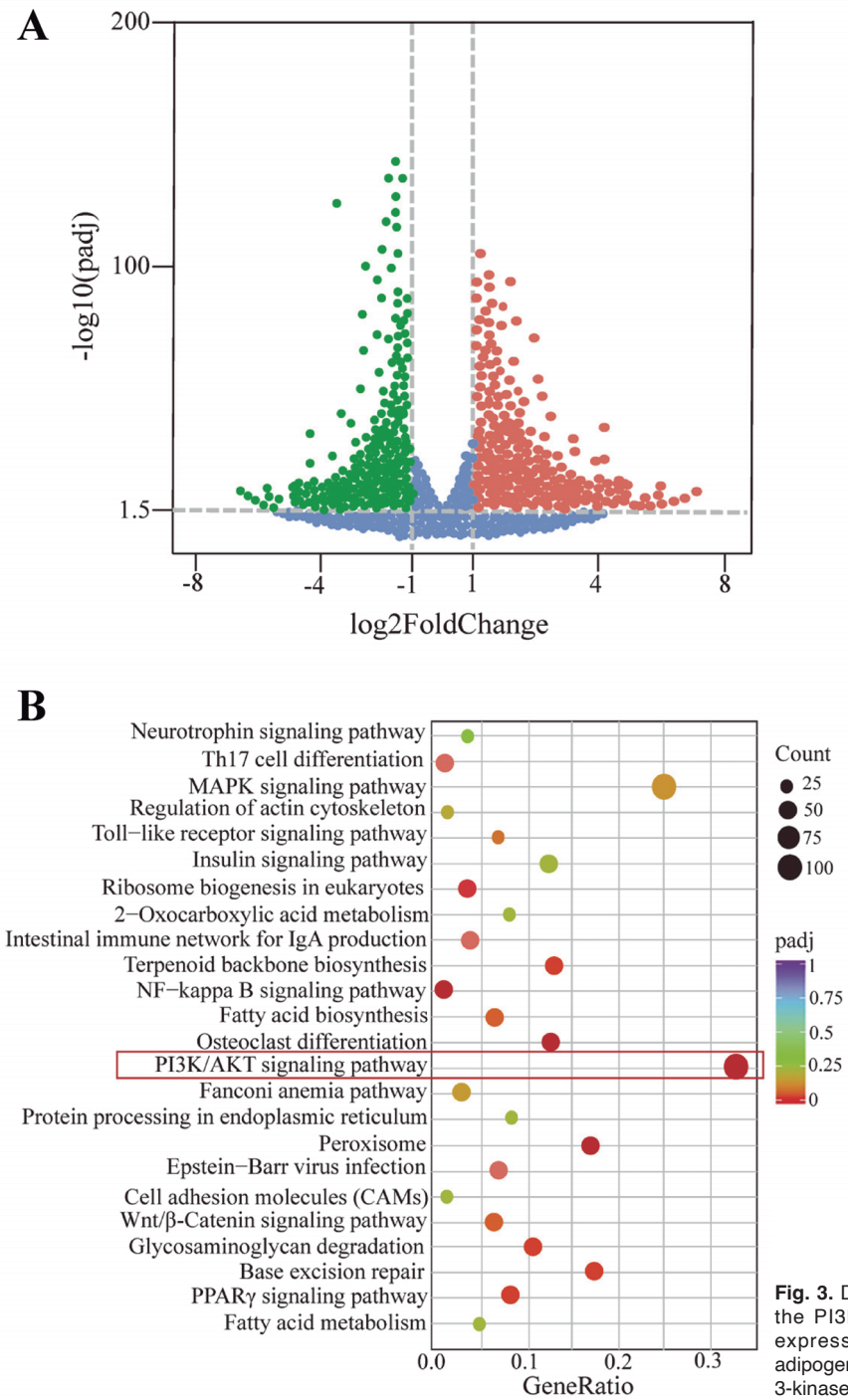

Fig. 3. D-mannose inhibited adipogenic differentiation through the PI3K/AKT signal pathway. **A.** Volcanic map of gene expression. **B.** Potential signaling pathway targeting on adipogenesis inhibition of D-mannose. PI3K: phosphoinositide 3-kinase.

than in Sham group (P<0.01), while the area of adipocytes and adipocyte area/tissue in the Mannose group were reduced (P<0.01). However, the area of adipocytes and adipocyte area/tissue area exhibited no significant differences between OVX and Fructose group.

Discussion

In our present study, we found that treatment with D-mannose inhibited adipogenesis of two representative hMSCs *in vitro* and inhibited adipogenesis of OVX rats *in vivo*. Mechanistically, D-mannose inhibited adipogenesis of hMSCs by restraining the PI3K/AKT pathway. Our results indicated the potential application of D-mannose, a safe nutritional supplement, in diseases related to excessive adipogenesis of MSCs such as obesity.

Obesity is caused by imbalance between adipogenesis and lipolysis, which eventually leads to the expansion of fat mass (Ludwig and Sorensen, 2022). Obesity, while it may seem common, can significantly shorten a person's life span because it increases the risk of metabolic diseases (Saltiel and Olefsky, 2017). Obesity is related to the over adipogenic differentiation of mesenchymal stem cells. This adipogenic differentiation process is regulated by the peroxidase proliferation-activated receptor (*PPARγ*) (Wang et al., 2022a) in orchestrating the expression of adipocyte-specific proteins, such as differential genes, including *C/EBPα* and *FABP4* (Wang et al., 2022b). Therefore, *PPARγ*, *C/EBPα* and *FABP4* are usually used as crucial markers to evaluate adipogenesis in our present research.

A large body of literature has demonstrated that D-

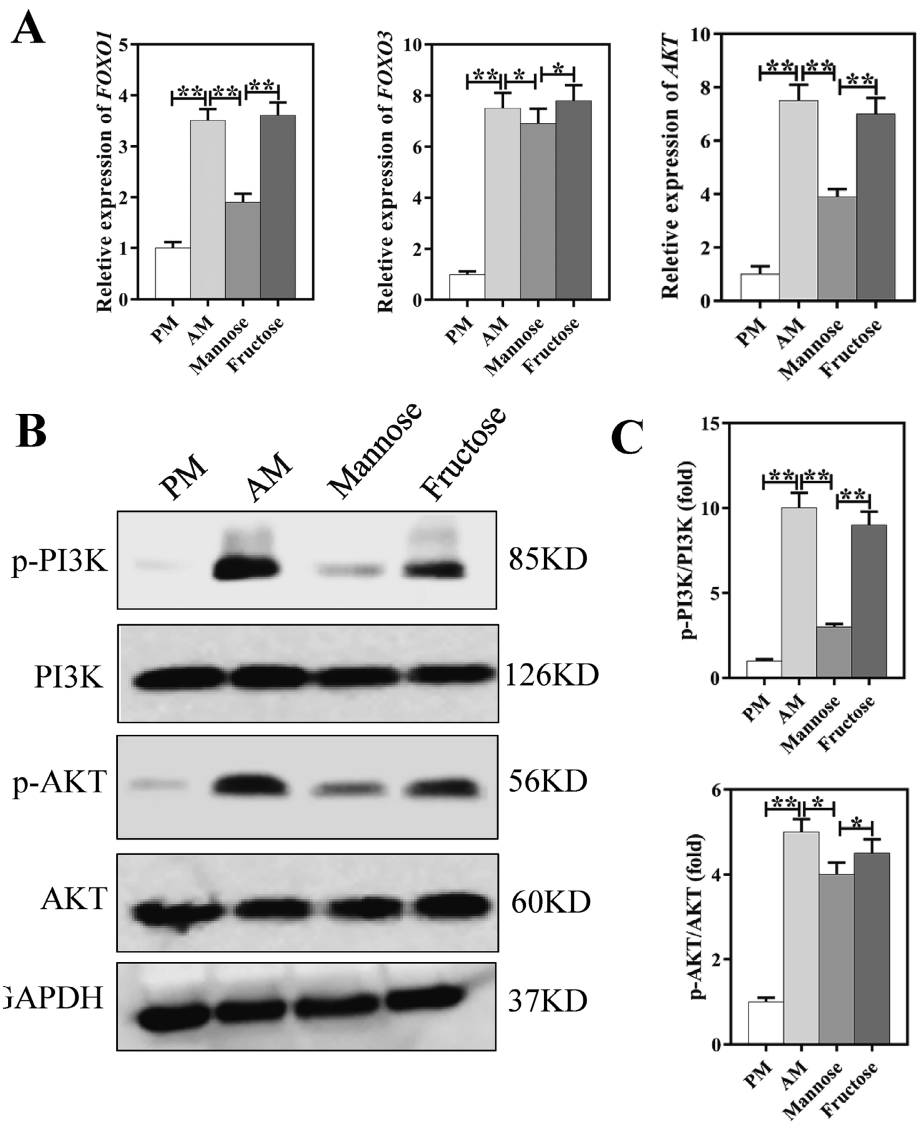

Fig. 4. D-mannose inhibited adipogenic differentiation of hADSCs through the PI3K/AKT signal pathway. **A.** Relative gene expression of FOXO1, FOXO3, and AKT for hADSCs treated with 25 mM D-mannose or D-fructose. **B.** Western blot figures of PI3K/AKT signal pathway expression for hADSCs. **C.** The statistical graph of p-PI3K/PI3K and p-AKT/AKT. **P*<0.05, ***P*<0.01. FOXO1: forkhead box protein 1; FOXO3: forkhead box protein 3; PI3K: phosphoinositide 3-kinase; p-PI3K: phospho- phosphoinositide 3-kinase.

mannose has a variety of beneficial physiological effects, such as anti-inflammatory (Lenger et al., 2020), immune regulation (Zhang et al., 2017), anti-tumor (Gonzalez et al., 2018), inhibition of bone resorption (Yang et al., 2022) and so on. Liu et al. recently found that D-mannose was able to inhibit adipogenic differentiation of adipose tissue-derived stem cells (hADSCs) (Liu et al., 2020b). Interestingly, Michaela et al. have reported that glucose was able to intensify the adipogenic differentiation of adipose-derived stem cells (Kolodziej et al., 2019). D-mannose, D-glucose, and D-fructose are all six-carbon sugars. So, in order to avoid the effect on adipogenic differentiation of D-glucose, we chose D-fructose as a control group.

We selected hADSCs as the representative cells and cultured D-mannose with concentrations of 0 mM, 10 mM, 25 mM and 50 mM. The influence of D-mannose with different concentrations on cell vitality was detected by CCK-8, and we found that D-mannose with different concentrations had little influence on cell vitality, which is shown in Fig 8. Therefore, 1.1 M D-mannose *in vivo* and 25 mM D-mannose *in vitro* were selected in our study. The concentration of D-mannose commonly used *in vitro* and *in vivo* in previous literature is summarized in Table 2.

Here we further proved that D-mannose inhibited adipogenic differentiation of both hADSCs and hBMSCs. In addition, through RNA-seq, we further found that the mechanism of D-mannose inhibiting adipogenesis was through the PI3K/AKT pathway. Also, qRT-PCR (the expression of target genes of *FOXO1*, *FOXO3*, and *AKT*) and WB (the expression of both phosphorylated and total protein of PI3K and AKT) were used to further verify the PI3K/AKT pathway. Besides, OVX rats were further used to explore the *in vivo* effects of D-mannose inhibiting adipogenesis.

Phosphoinositide 3-kinase (PI3K) was firstly discovered by Whitman et al. (1985). PI3K/AKT

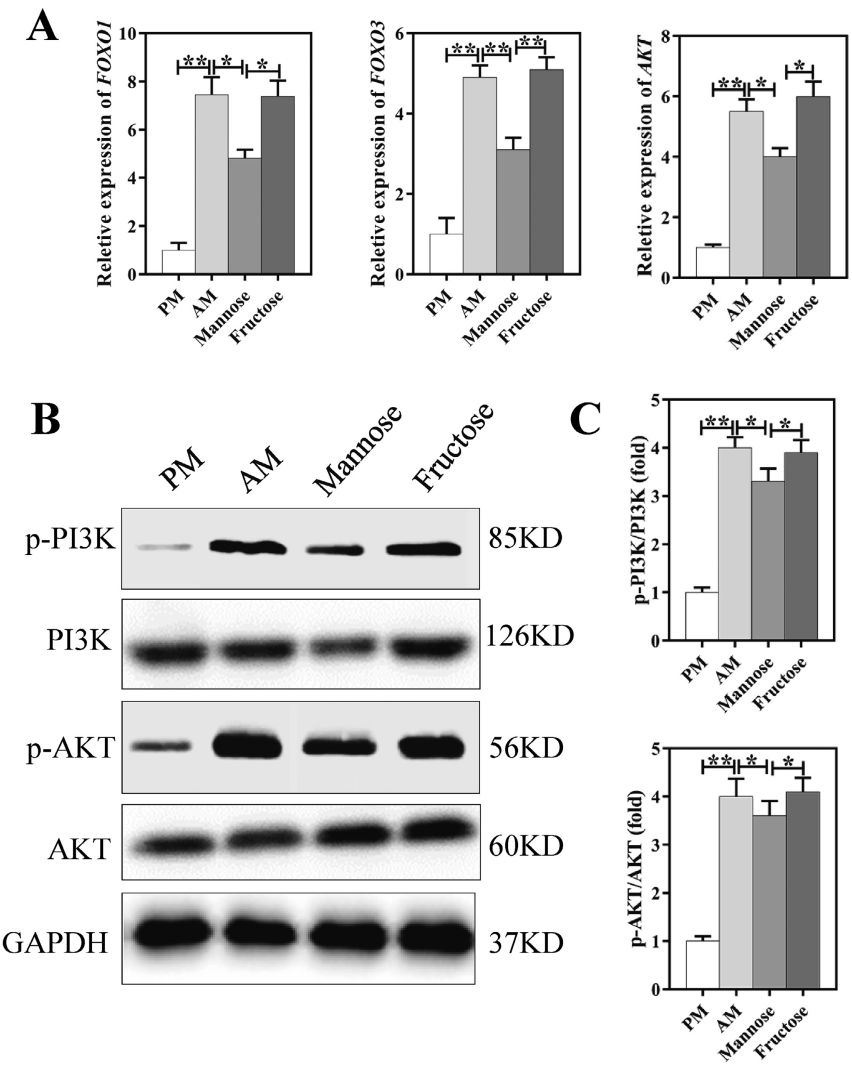

Fig. 5. D-mannose inhibited adipogenic differentiation of hBMSCs through the PI3K/AKT signal pathway. **A.** Relative gene expression of FOXO1, FOXO3, and AKT for hBMSCs treated with 25 mM D-mannose or D-fructose. **B.** Western blot figures of PI3K/AKT signal pathway expression for hBMSCs. **C.** The statistical graph of p-PI3K/PI3K and p-AKT/AKT. **P*<0.05, ***P*<0.01. FOXO1: forkhead box protein 1; FOXO3: forkhead box protein 3; FABPA: adipocyte fatty acid-binding protein α; PI3K: phosphoinositide 3-kinase; p-PI3K: phospho- phosphoinositide 3-kinase.

signaling plays an important role in cellular physiology in glucose homeostasis, lipid metabolism, and protein synthesis (Abeyrathna and Su, 2015). Previous studies have revealed that PI3K/AKT signaling was increased during adipogenic differentiation (Nakae et al., 2003). Our present results are consistent with those of the previous studies, and we firstly point out that D-mannose inhibits adipogenesis both *in vitro* and *in vivo* through the PI3K/AKT pathway. Although the specific mechanism of how D-mannose inhibits adipogenesis of hMSCs has not been completely understood, in our present study, it is mediated, at least partly, by inhibiting the PI3K/AKT signal pathway.

Nevertheless, there exist several limitations of our present study. We only initially explored the effect of different concentrations of D-mannose on proliferation of hADSCs by CCK-8. Referring to previous studies (Zhang et al., 2017), we mainly studied the effect of 25 mM D-mannose on adipogenesis, and did not conduct a more in-depth study of D-mannose with different concentration gradients. As a kind of safe natural product, D-mannose exerted its biological effects at concentrations in a wide range (Liu et al., 2020a). However, further exploration is needed to determine the exact effective concentrations for humans if our present result, i.e., D-mannose inhibits adipogenesis, is to be used in clinical applications for the treatment of obesity.

In short, our results indicate that D-mannose can restrain the adipogenesis of hADSCs and hBMSCs *in vitro* and *in vivo* by suppressing the PI3K/AKT signal pathway. These results suggest that D-mannose is effective and safe in regulating adipogenesis of mesenchymal stem cells. Therefore D-mannose can act as a potential therapeutic option with minimal side effects to treat diseases related to excessive adipogenic differentiation of MSCs such as obesity.

Table 2. The concentration of D-mannose used in previous studies.

in vitro /*in vivo*	cell/animal	concentration	intervention	Reference
in vivo	C57BL/6 mice	1.1 M/L	dissolved in water	Zhang et al., 2017
in vivo	C57BL/6 mice	1.1 M/L	dissolved in water	Ito et al., 2022
in vivo	C57BL/6 mice	w/v=20%	dissolved in water	Davis and Freeze, 2001
in vivo	C57BL/6 mice	450 mg/kg	intraperitoneal injection	Wang et al., 2021a
in vitro	T cells	25 mM/L	dissolved in medium	Zhang et al., 2017
in vitro	mice bone marrow monocytes	25 mM/L	dissolved in medium	Torretta et al., 2020
in vitro	MDA-MB-231	25 mM/L	dissolved in medium	Zhang et al., 2022
in vitro	mice bone marrow monocytes	0 mM/L; 1 mM/L; 10 mM/L; 50 mM/L	dissolved in medium	Wang et al., 2021a
in vitro	bone marrow dendritic cells	10 mM/L	dissolved in medium	Wang et al., 2021b
in vitro	keratinocytes	10 mM/L	dissolved in medium	Luo et al., 2022

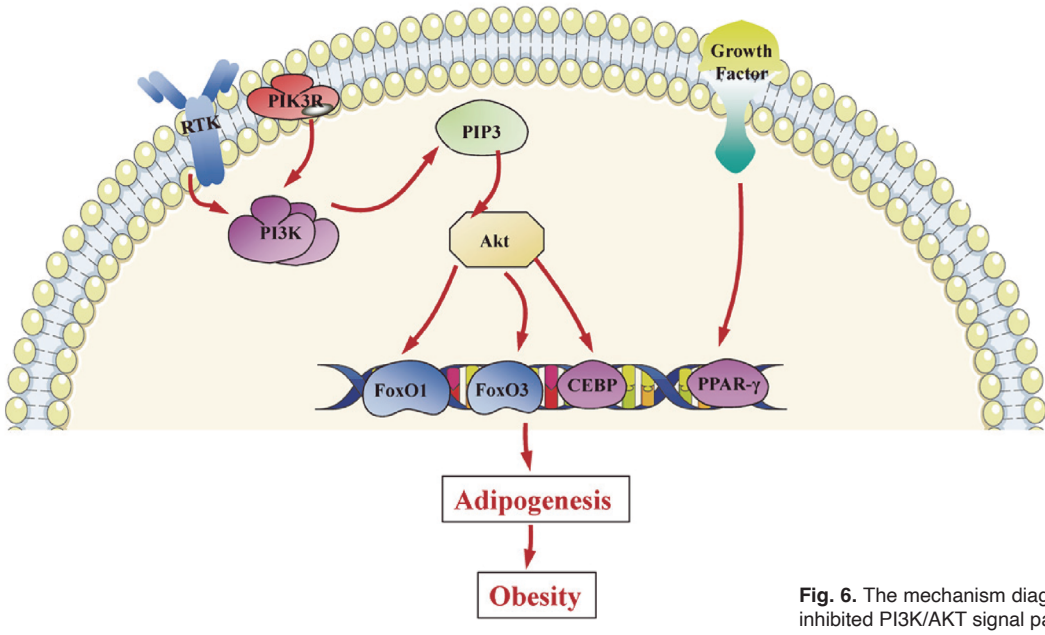

Fig. 6. The mechanism diagrammatic drawing of D-mannose inhibited PI3K/AKT signal pathway.

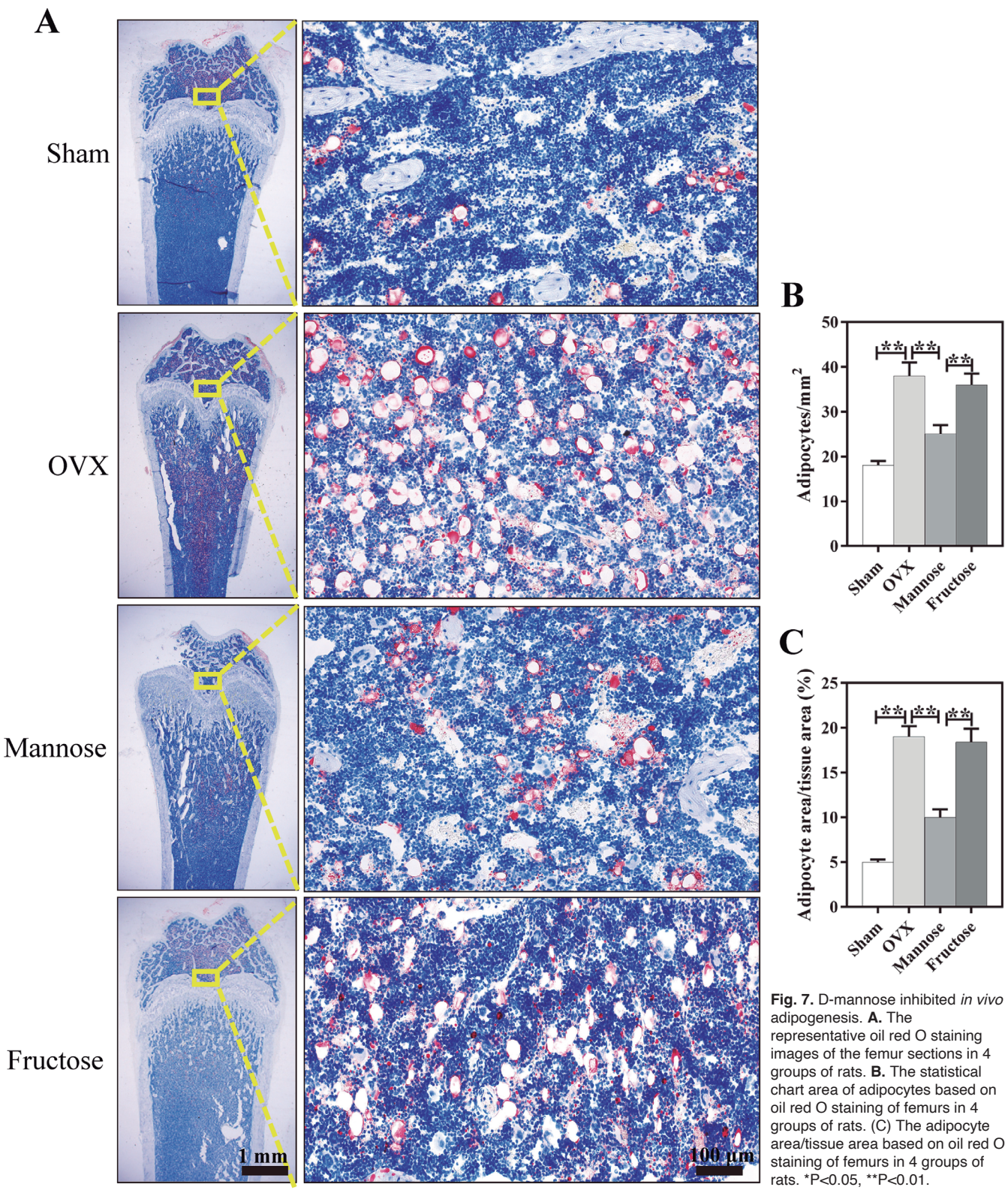

Fig. 7. D-mannose inhibited *in vivo* adipogenesis. **A.** The representative oil red O staining images of the femur sections in 4 groups of rats. **B.** The statistical chart area of adipocytes based on oil red O staining of femurs in 4 groups of rats. (C) The adipocyte area/tissue area based on oil red O staining of femurs in 4 groups of rats. *P<0.05, **P<0.01.

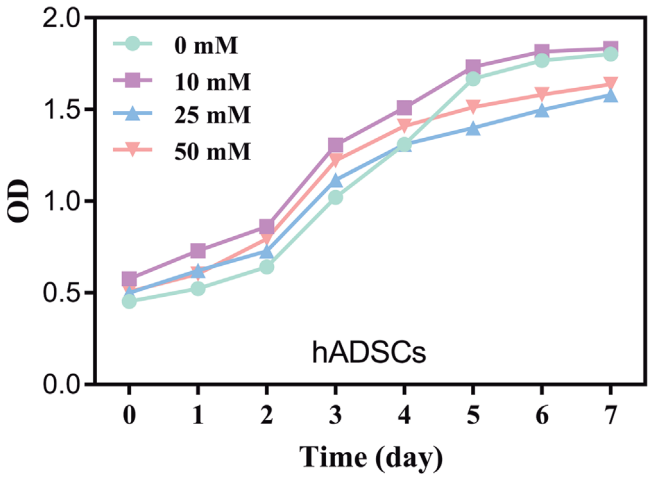

Fig. 8. The proliferation curve of hADSCs treated with different concentrations of D-mannose.

Acknowledgements. This work was supported by the Youth Research Fund of Affiliated Hospital of Qingdao University (grant number: QDFYQN20190028).

Declaration of competing interest. All authors declared that they have no competing financial interests.

Authors' roles. Study design: HZL and CG. Study conduct: HZL, LW, and YZL. Data collection: XL and JPZ. Data analysis: XL and JPZ. Data interpretation: HZL and CG. Drafting manuscript: HZL and CG. Revising manuscript content: HZL, LW, YZL, JPZ, XL and CG. Approving final version of manuscript: HZL, LW, YZL, JPZ, XL and CG. CG takes responsibility for the integrity of data analysis.

References

Abeyrathna P. and Su Y. (2015). The critical role of Akt in cardiovascular function. Vascul. Pharmacol. 74, 38-48.

Aherne W. and Hull D. (1966). Brown adipose tissue and heat production in the newborn infant. J. Pathol. Bacteriol. 91, 223-234.

Davis J.A. and Freeze H.H. (2001). Studies of mannose metabolism and effects of long-term mannose ingestion in the mouse. Biochim. Biophys. Acta 1528, 116-126.

Ducy P., Desbois C., Boyce B., Pinero G., Story B., Dunstan C., Smith E., Bonadio J., Goldstein S., Gundberg C., Bradley A. and Karsenty G. (1996). Increased bone formation in osteocalcin-deficient mice. Nature 382, 448-452.

Ghaben A.L. and Scherer P.E. (2019). Adipogenesis and metabolic health. Nat. Rev. Mol. Cell Biol. 20, 242-258.

Gonzalez P.S., O'Prey J., Cardaci S., Barthet V.J.A., Sakamaki J.-I., Beaumatin F., Roseweir A., Gay D.M., Mackay G., Malviya G., Kania E., Ritchie S., Baudot A.D., Zunino B., Mrowinska A., Nixon C., Ennis D., Hoyle A., Millan D., McNeish I.A., Sansom O.J., Edwards J. and Ryan K.M. (2018). Mannose impairs tumour growth and enhances chemotherapy. Nature 563, 719-723.

Green H. and Meuth M. (1974). An established pre-adipose cell line and its differentiation in culture. Cell 3, 127-133.

Guo L., Hou Y., Song L., Zhu S., Lin F. and Bai Y. (2018). D-Mannose enhanced immunomodulation of periodontal ligament stem cells via inhibiting IL-6 secretion. Stem Cells Int. 2018, 7168231.

Haywood C. and Sumithran P. (2019). Treatment of obesity in older persons-A systematic review. Obes. Rev. 20, 588-598.

Ito D., Ito H., Ideta T., Kanbe A. and Shimizu M. (2022). D-mannose administration improves autoimmune hepatitis by upregulating regulatory T cells. Cell Immunol. 375, 104517.

Jackson V.M., Breen D.M., Fortin J.-P., Liou A., Kuzmiski J.B., Loomis A.K., Rives M.L., Shah B. and Carpino P.A. (2015). Latest approaches for the treatment of obesity. Expert Opin. Drug Discov. 10, 825-839.

Kolodziej M., Strauss S., Lazaridis A., Bucan V., Kuhbier J.W., Vogt P.M. and Konneker S. (2019). Influence of glucose and insulin in human adipogenic differentiation models with adipose-derived stem cells. Adipocyte 8, 254-264.

Kyriakides R., Jones P. and Somani B.K. (2021). Role of D-mannose in the prevention of recurrent urinary tract infections: Evidence from a systematic review of the literature. Eur. Urol. Focus 7, 1166-1169.

Lenger S.M., Bradley M.S., Thomas D.A., Bertolet M.H., Lowder J.L. and Sutcliffe S. (2020). D-mannose vs other agents for recurrent urinary tract infection prevention in adult women: a systematic review and meta-analysis. Am. J. Obstet. Gynecol. 223, 265 e261-265 e213.

Liu H., Gu R., Zhu Y., Lian X., Wang S., Liu X., Ping Z., Liu Y. and Zhou Y. (2020a). D-mannose attenuates bone loss in mice via Treg cell proliferation and gut microbiota-dependent anti-inflammatory effects. Ther. Adv. Chronic Dis. 11, 2040622320912661.

Liu Y., Guo L., Hu L., Xie C., Fu J., Jiang Y., Han N., Jia L. and Liu Y. (2020b). D-mannose inhibits adipogenic differentiation of adipose tissue-derived stem cells via the miR669b/MAPK athway. Stem Cells Int. 2020, 8866048.

Ludwig D.S. and Sorensen T.I.A. (2022). An integrated model of obesity pathogenesis that revisits causal direction. Nat. Rev. Endocrinol. 18, 261-262.

Luo J., Li Y., Zhai Y., Liu Y., Zeng J., Wang D., Li L., Zhu Z., Chang B., Deng F., Zhang J., Zhou J. and Sun L. (2022). D-Mannose ameliorates DNCB-induced atopic dermatitis in mice and TNF-alpha-induced inflammation in human keratinocytes via mTOR/NF-kappaB pathway. Int. Immunopharmacol. 113(Pt A): 109378.

Murina F., Vicariotto F. and Lubrano C. (2021). Efficacy of an orally administered combination of Lactobacillus paracasei LC11, cranberry and D-mannose for the prevention of uncomplicated, recurrent urinary tract infections in women. Urologia 88, 64-68.

Nakae J., Kitamura T., Kitamura Y., Biggs 3rd W.H., Arden K.C. and Accili D. (2003). The forkhead transcription factor Foxo1 regulates adipocyte differentiation. Dev. Cell 4, 119-129.

Piche M.E., Tchernof A. and Despres J.-P. (2020). Obesity phenotypes, diabetes, and cardiovascular diseases. Circ. Res. 126, 1477-1500.

Rathmell J.C. (2021). Obesity, immunity, and cancer. N. Engl. J. Med. 384, 1160-1162.

Saltiel A.R. and Olefsky J.M. (2017). Inflammatory mechanisms linking obesity and metabolic disease. J. Clin. Invest. 127, 1-4.

Sharma V., Smolin J., Nayak J., Ayala J.E., Scott D.A., Peterson S.N. and Freeze H.H. (2018). Mannose alters gut microbiome, prevents diet-induced obesity, and improves host metabolism. Cell Rep. 24, 3087-3098.

Torretta S., Scagliola A., Ricci L., Mainini F., Di Marco S., Cuccovillo I., Kajaste-Rudnitski A., Sumpton D., Ryan K.M. and Cardaci S. (2020). D-mannose suppresses macrophage IL-1β production. Nat.

Commun. 11, 6343.

Wang J., Motlagh N.J., Wang C., Wojtkiewicz G.R., Schmidt S., Chau C., Narsimhan R., Kullenberg E.G., Zhu C., Linnoila J., Yao Z. and Chen J.W. (2021a). D-mannose suppresses oxidative response and blocks phagocytosis in experimental neuroinflammation. Proc. Natl. Acad. Sci. USA 118, e2107663118.

Wang H., Teng X., Abboud G., Li W., Ye S. and Morel L. (2021b). D-mannose ameliorates autoimmune phenotypes in mouse models of lupus. BMC Immunol. 22, 1.

Wang S., Lin Y., Gao L., Yang Z., Lin J., Ren S., Li F., Chen J., Wang Z., Dong Z., Sun P. and Wu B. (2022a). PPAR-γ integrates obesity and adipocyte clock through epigenetic regulation of Bmal1. Theranostics 12, 1589-1606.

Wang X. W., Sun Y.J., Chen X. and Zhang W.-Z. (2022b). Interleukin-4-induced FABP4 promotes lipogenesis in human skeletal muscle cells by activating the PPAR γ signaling pathway. Cell Biochem. Biophys. 80, 355-366.

Whitman, M., Kaplan D.R., Schaffhausen B., Cantley L. and Roberts T.M. (1985). Association of phosphatidylinositol kinase activity with polyoma middle-T competent for transformation. Nature 315, 239-242.

Yang H., Han N., Luo Z., Xu J., Guo L. and Liu Y. (2022). D-Mannose alleviated alveolar bone loss in experimental periodontitis mice via regulating the anti-inflammatory effect of amino acids. J. Periodontol. 94, 542-553.

Zhang D., Chia C., Jiao X., Jin W., Kasagi S., Wu R., Konkel J.E., Nakatsukasa H., Zanvit P., Goldberg N., Chen Q., Sun L., Chen Z.-J. and Chen W. (2017). D-mannose induces regulatory T cells and suppresses immunopathology. Nat. Med. 23, 1036-1045.

Zhang R., Yang Y., Dong W., Lin M., He J., Zhang X., Tian T., Yang Y., Chen K., Lei Q.Y., Zhang S., Xu Y. and Lv L. (2022). D-mannose facilitates immunotherapy and radiotherapy of triple-negative breast cancer via degradation of PD-L1. Proc. Natl. Acad. Sci. USA 119, 119, e2114851119.

Zhou X., Zheng Y., Sun W., Zhang Z., Liu J., Yang W., Yuan W., Yi Y., Wang J. and Liu J. (2021). D-mannose alleviates osteoarthritis progression by inhibiting chondrocyte ferroptosis in a HIF-2alpha-dependent manner. Cell Prolif. 54, e13134.

Accepted May 23, 2023